

NATIONAL RADIO ASTRONOMY OBSERVATORY

Engineering Memo No. 133

HIGH FREQUENCY PERFORMANCE OF THE 140-FOOT TELESCOPE
II. OBSERVATIONS AT 22,235 MHz

Robert L. Brown
October 1979

I. 22,235 MHz Observations

As part of a continuing effort to understand the high frequency characteristics of the 140-foot telescope, I undertook the series of astronomical observations described below at 22,235 MHz (1.345 cm). The purpose of the observations was to determine the relative telescope sensitivity, Jy/K, as a function of hour angle and source declination and to compare these results with a similar set of measurements made at 10,522 MHz (Engineering Memo No. 132).

The present observations differ from those I made at 10.5 GHz in several respects. Perhaps most importantly, at 22 GHz it is difficult to obtain an absolute set of measurements because there are few compact, strong, continuum sources in the sky for which absolute fluxes are well determined. There are 3 such sources, however, 3C 84 ($\delta = 42^\circ$), 3C 274 ($\delta = 12^\circ$) and 3C 273 ($\delta = 2^\circ$) and all these were observed. At other declinations it is possible to use H₂O masers as narrow band continuum sources. The advantage in using strong maser sources is that measurements of high signal-to-noise are readily obtained; the disadvantage is that an absolute measurement of the telescope aperture efficiency cannot be made because the flux density of the maser-line sources averaged over the bandpass is unknown. In the latter case only a relative efficiency can be determined.

The 22 GHz observations also differ from the 10 GHz observations in that the former were all made at the Cassegrain focus whereas the latter were made

at the prime focus. The distinction here involves more than simply the introduction of a subreflector into the optics: in all the observations described below (the few exceptions are explicitly noted) the subreflector was dynamically deformed under computer control so as to correct for the gravitational deformation of the telescope (cf. Engineering Memo No. 109). In this regard it is important to note that the purpose of the deforming action of the subreflector is not to improve the zenith aperture efficiency of the telescope, rather it is to improve the efficiency at points away from the zenith (cf. Engineering Memo No. 108-9). In section VI, I briefly evaluate the success of the present deforming subreflector in achieving this goal.

All the observations were made during the second and third weeks of September 1979. The weather throughout the run was nearly perfect; such conditions minimized the sky contribution at 22 GHz and allowed us to obtain a typical system temperature of 55-70 K. The receiver performed flawlessly. All the observations were made by first moving the telescope to the source and positioning the telescope directly on source by means of the on-line telescope routine PEAK. Next the source temperature was measured by means of a repeated series of ON-OFF measurements followed by a calibration scan with the noise tube on. Lastly, a system temperature measurement was made off source so that an estimate could be made of the atmospheric attenuation. All these measurements were made with the telescope under card control using the routine VSST. The telescope operator was required only to update the subreflector's deformation and to turn on and off the nutator (ON for pointing and source temperature measurements, OFF for system temperature measurements).

The sources I observed, and their respective 22,235 MHz continuum flux densities (when applicable) are given in the table below.

TABLE 1
Source Parameters

Source	Declination	22,235 MHz Flux Density (Jy)	Notes
W3 (OH)	61° 38'	H ₂ O Maser	
3C 84	41° 19'	34.0	1
3C 274	12° 40'	20.0	2
W49	09° 01'	H ₂ O Maser	
3C 273	02° 19'	19.0	1
W43	-01° 57'	H ₂ O Maser	
Orion A	-05° 24'	H ₂ O Maser	
W31	-19° 56'	H ₂ O Maser	
Sgr-B2	-28° 22'	H ₂ O Maser	

Notes:

1. 1.3 cm flux density from the Bonn list of fundamental calibrators.
2. 1.3 cm flux density obtained at the VLA courtesy of Ed Fomalont.

II. Results: Relative Telescope Sensitivity as a Function of Hour Angle

In an attempt to determine the relative variation in telescope aperture efficiency, or equivalently K/Jy, with hour angle, I normalized the source temperature measurements for each source to the maximum observed source antenna temperature. The resulting degradation as a function of hour angle is then readily displayed. Figures 1(a) to 1(g) illustrate this relative change in telescope sensitivity for seven of the sources listed in table 1; the sources cover the full range of declinations +60° to -30°. Several conclusions are apparent from this data:

- (1) The 1.3 cm performance of the telescope is a strong function of hour angle at all declinations.
- (2) The point of maximum sensitivity is east of the meridian at all declinations.
- (3) The point of maximum sensitivity is furthest east ($\sim 2^{\text{h}} 20^{\text{m}}$) for sources at very high declinations; this point moves uniformly west (toward the meridian) for sources at lower declinations; at -30° declination the point of maximum sensitivity is only $\sim 20^{\text{min}}$ east.

Conclusions (2) and (3) are simply a restatement of the 140-foot "asymmetry", an effect known to be present at other wavelengths as well. Moreover, the magnitude as well as the sense of the asymmetry is the same at 22 GHz as at 10 GHz--at 10 GHz also the shift of maximum sensitivity is more than 2^{h} east at $\delta = 60^\circ$ while at $\delta < 0^\circ$ it is only about 15^{m} east. This latter correlation is important because it means that the cause of the "asymmetry" is something common in all respects to both the prime focus and the Cassegrain focus. Von Hoerner's conclusion, therefore, that the asymmetry is related to a lateral displacement of the feed (or the center of the subreflector) from the electrical axis of the telescope is quite likely correct (Engineering Memo No. 130).

III. 140-Foot Aperture Efficiency at 22,235 MHz

Fortunately, it is possible to obtain the absolute zenith K-band aperture efficiency of the 140-foot from the observation of a source, 3C 84, which passes very nearly through the zenith. Using the flux density of 3C 84 given in Table 1, I have used the data of Figure 1b to determine the telescope aperture efficiency at 22,235 MHz; these results are shown in Figure 2. Also presented on this same figure are the corresponding measurements of the same source made at 10,522 MHz (Engineering Memo No. 132).

The peak aperture efficiency of the 140-foot telescope at 22,235 MHz is 23%. This is approximately half the peak aperture efficiency at 10,522 MHz.

The variation of the peak 22 GHz aperture efficiency with declination is very slight--at least from +40° to 0° declination. This can be seen from the measurements of 3C 84, 3C 274 and 3C 273:

3C 84	$\delta = +42^\circ$	$\eta = 23.2\%$
3C 274	$\delta = +12^\circ$	$\eta = 20.1\%$
3C 273	$\delta = + 2^\circ$	$\eta = 20.5\%$

Here it is important to recall that the deforming subreflector was used in all these measurements.

IV. RMS Surface Roughness of the 140-Ft.

If we assume that the lower peak aperture efficiency of the telescope found at 22,235 MHz relative to the long wavelength aperture efficiency is due entirely to small, uncorrelated, surface non-uniformities, then we may make use of Ruze's expression and solve for the surface rms roughness σ ,

$$\eta(\lambda) = \eta(\lambda = \infty) \exp [-0.75 (4\pi\sigma/\lambda)^2].$$

For $\eta(\lambda = \infty) = 0.53$ and $\eta(1.345 \text{ cm}) = 0.23$, we find $\sigma(\text{rms}) = 1.12 \text{ mm}$. This number compares favorably with Findlay's measurements of the surface in which he derives a mean $\sigma(\text{rms}) = 1.26 \text{ mm}$ (Engineering Memo No. 129).

V. Variations in the Telescope Beam Shape with Hour Angle

It is perhaps no surprise that the rapid variation of telescope sensitivity with hour angle is accompanied by a change in telescope beam shape. Measurements by Turner and Rickard with the fixed subreflector showed this effect dramatically. Now with the deforming subreflector the situation is improved somewhat (particularly in the east) but the overall trend is still present.

To illustrate the trend with hour angle, I followed 3C 273 (declination $+2^\circ$) across the sky mapping the beam every 30 minutes. Nine of these maps running from $3^{\text{h}} 30^{\text{m}}$ East to $3^{\text{h}} 10^{\text{m}}$ West are shown as Figures 3(a) to 3(c). For all these observations the deforming subreflector was used. Here it can be seen that in the far east the beam is reasonably well defined but [Figure 1d or 1e] it is clear that considerable power ($\sim 40\%$) is missing from the main beam and that the missing power must be in an extended lobe, not a nearby sidelobe. Going from the east toward the meridian the beam becomes increasingly well defined--at least up to $0^{\text{h}} 50^{\text{m}}$ East. On the meridian a ~ 10 db sidelobe forms $\sim 2'$ from the main beam. Further west this sidelobe continues to grow at the expense of the main beam, and soon is joined ($\sim 2^{\text{h}}$ West) by another sidelobe on the opposite side of the main beam. Far west, $2^{\text{h}} 30^{\text{m}}$ West or more, reference to the "main beam" becomes ambiguous.

In these figures the "telescope asymmetry" is readily apparent--compare, for instance, the beam $2^{\text{h}} 00^{\text{m}}$ east with that $2^{\text{h}} 20^{\text{m}}$ west.

VI. Effectiveness of the Deforming Subreflector

In order to assess the effect the deforming subreflector has on the telescope aperture efficiency, I followed a number of sources across the sky and measured their antenna temperature both with the subreflector deforming under computer control and also with the subreflector locked in the undeformed position. The results for 3C 273 are shown on Figure 4. Here it can be seen that the subreflector as deformed provides some improvement in telescope aperture efficiency over the whole sky, but the improvement is very marked in the east.

Perhaps more graphically one can see these same results from beam maps. In Figure 5 I show the telescope beam for 3C 273 at $0^{\text{h}} 20^{\text{m}}$ West for both cases:

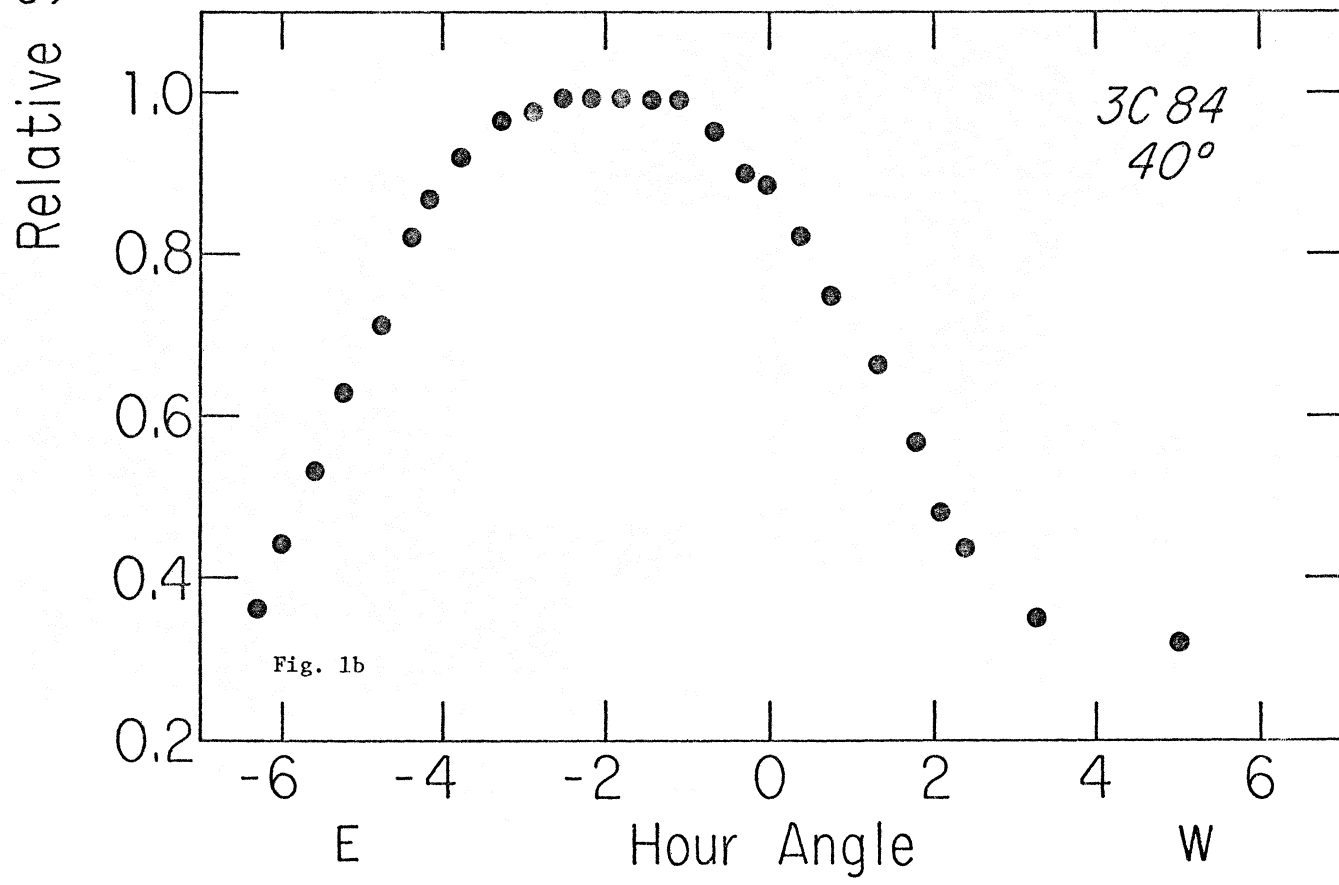
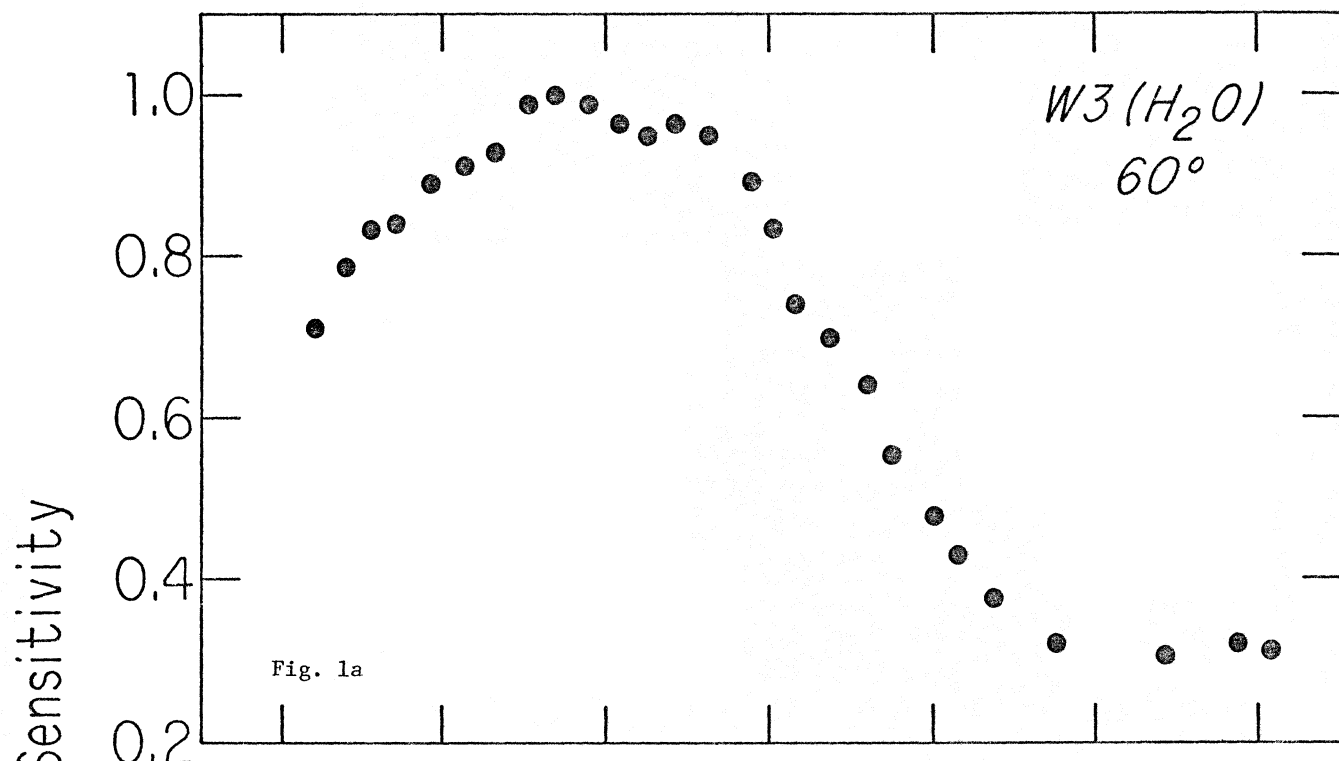
when the subreflector is locked in an undeformed position (Figure 5a), and when the subreflector is allowed to deform to its proper shape. Figure 6 is a similar illustration for the same source $2^{\text{h}} 20^{\text{m}}$ West. In this latter case it can be seen that although the deforming subreflector allows some improvement it is clear that effects other than gravitational astigmatism are dominating the telescope performance.

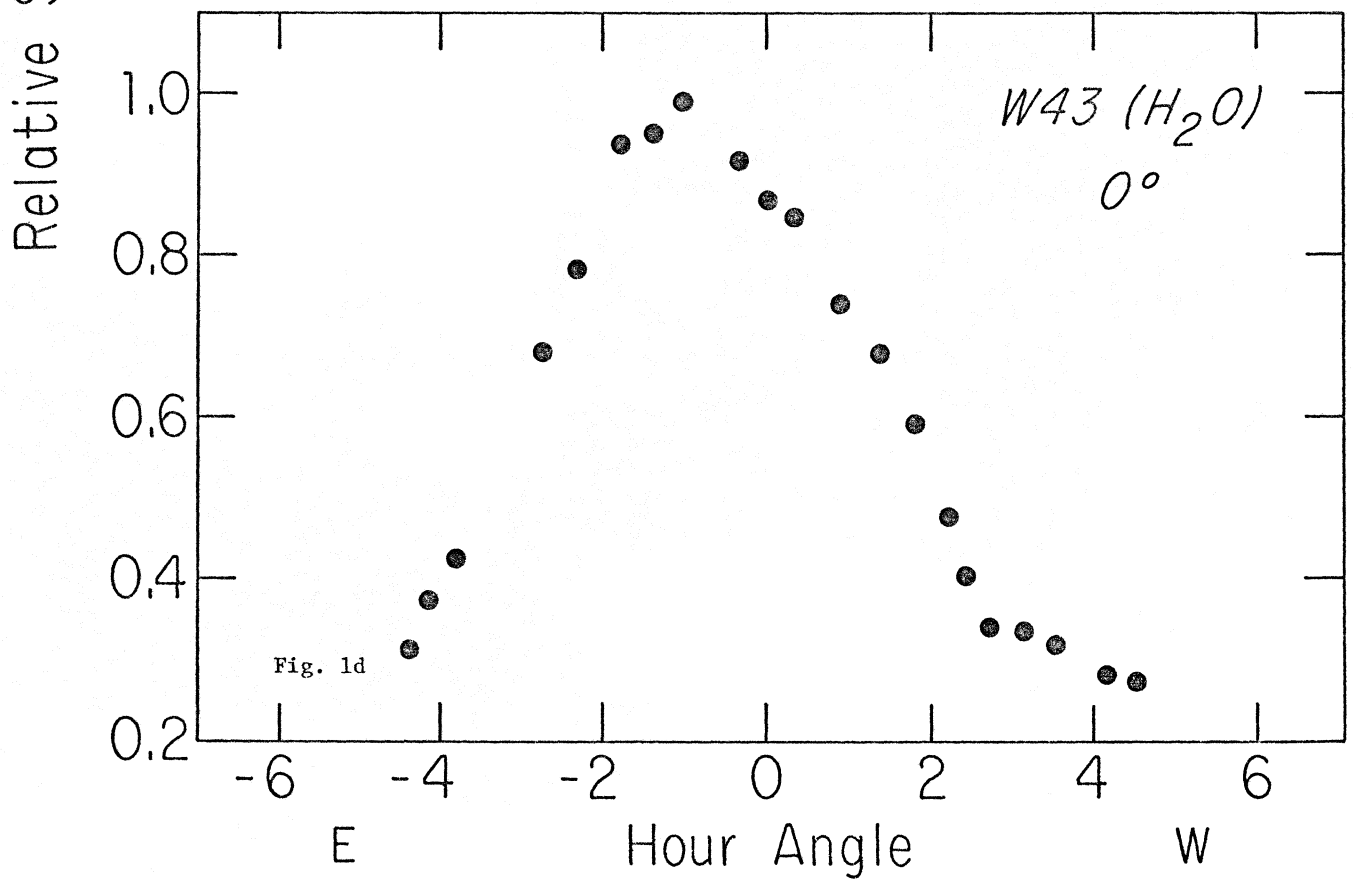
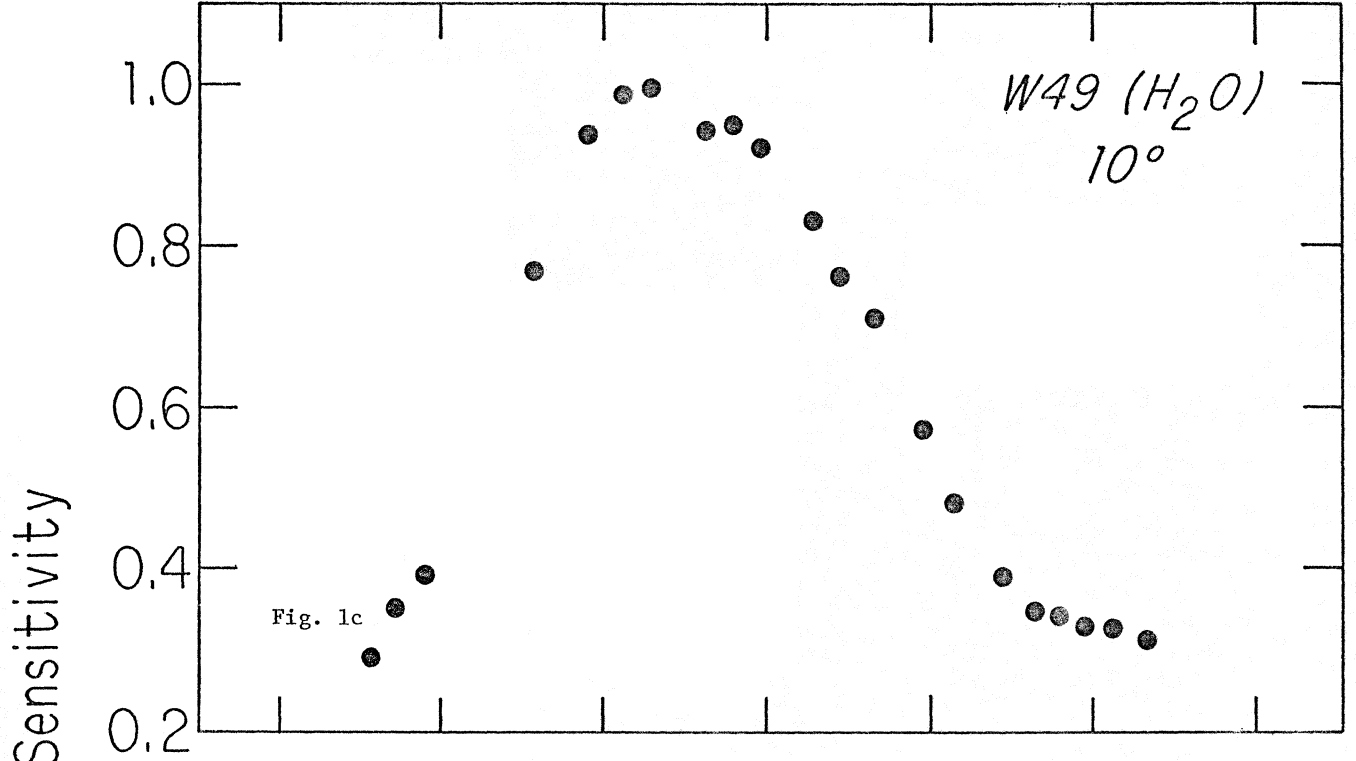
VII. Improvements

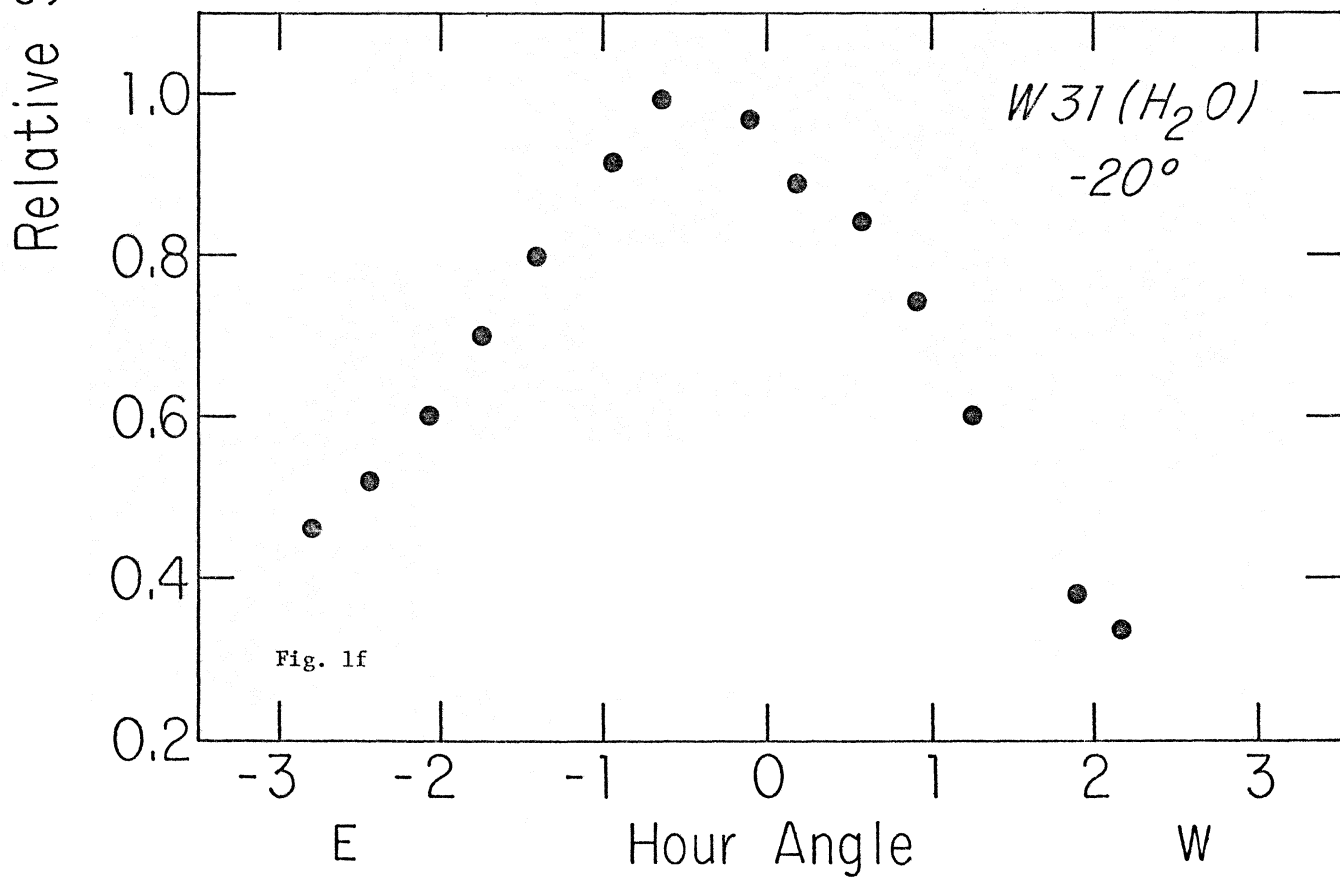
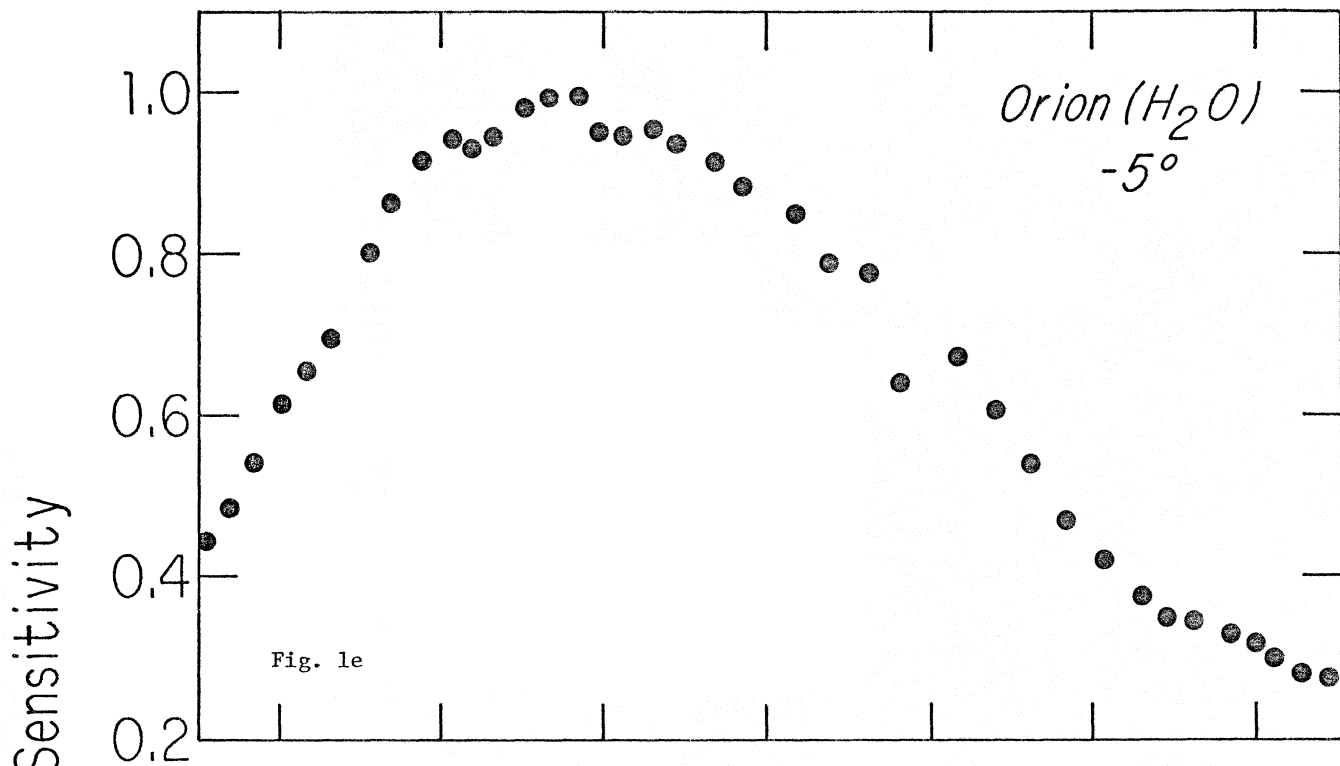
1. Although the solution to the telescope asymmetry is likely to be found with a new Sterling mount which will allow an east-west lateral movement (von Hoerner: Engineering Memo No. 130), such a replacement is a major undertaking. As an interim measure the center of the present Sterling mount will be moved more nearly on the electrical axis of the telescope. At the conclusion of this work (planned for January 1979) the 22,235 MHz measurements should be repeated.

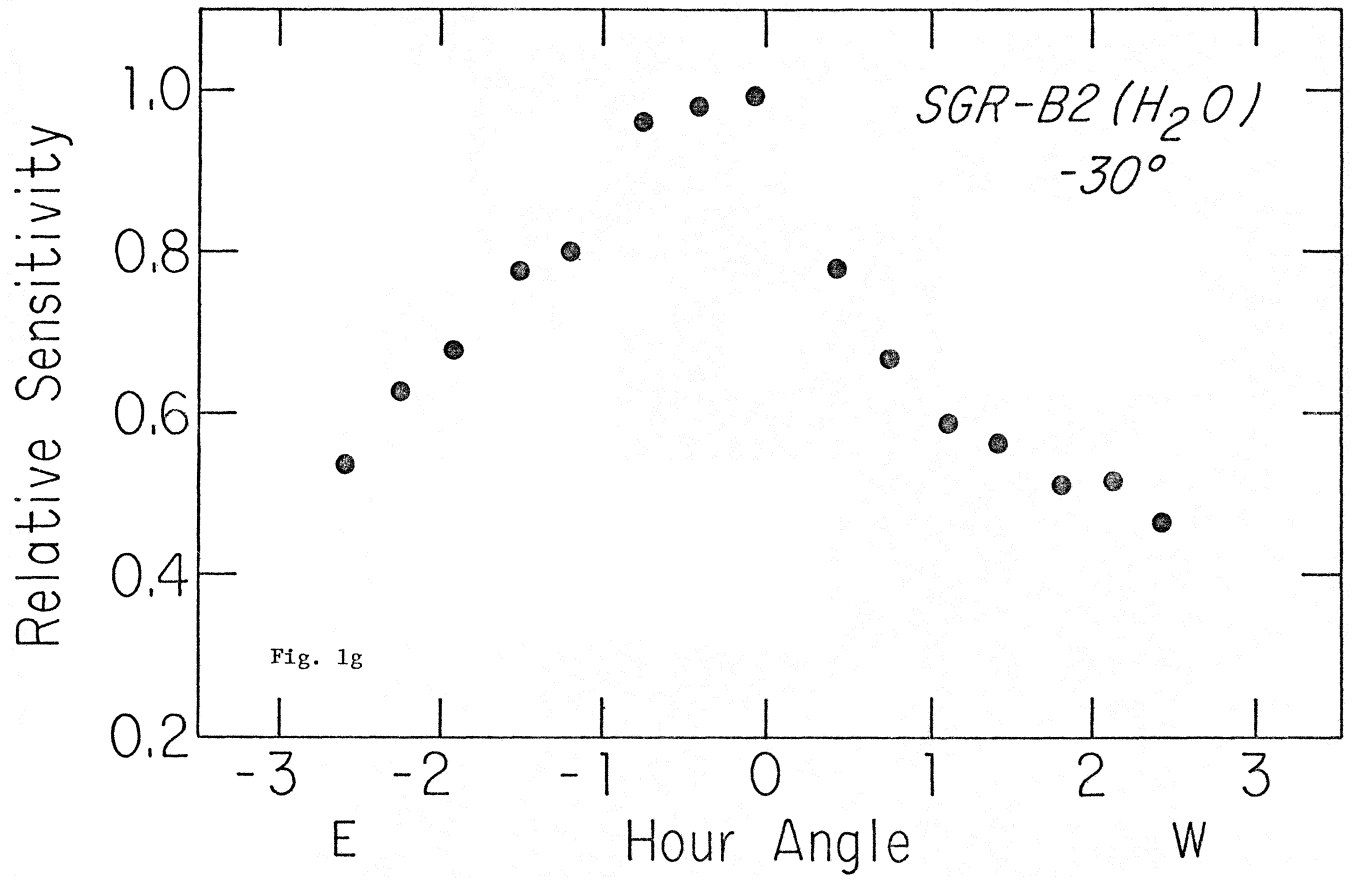
2. The deforming subreflector provides a substantial improvement in telescope performance over much of the sky. However, for the measurements described above the subreflector could not be deformed for the design amount at low elevations ($\sim 35^\circ$ elevation) because the actuating motors lacked sufficient travel. Replacement of these actuators with proper ones (Fall 1979) is a necessary step which promises even better performance on low declination sources.

3. Upon the completion and evaluation of (1) and (2), the feasibility and desirability of resetting and/or upgrading the telescope surface should be considered anew.









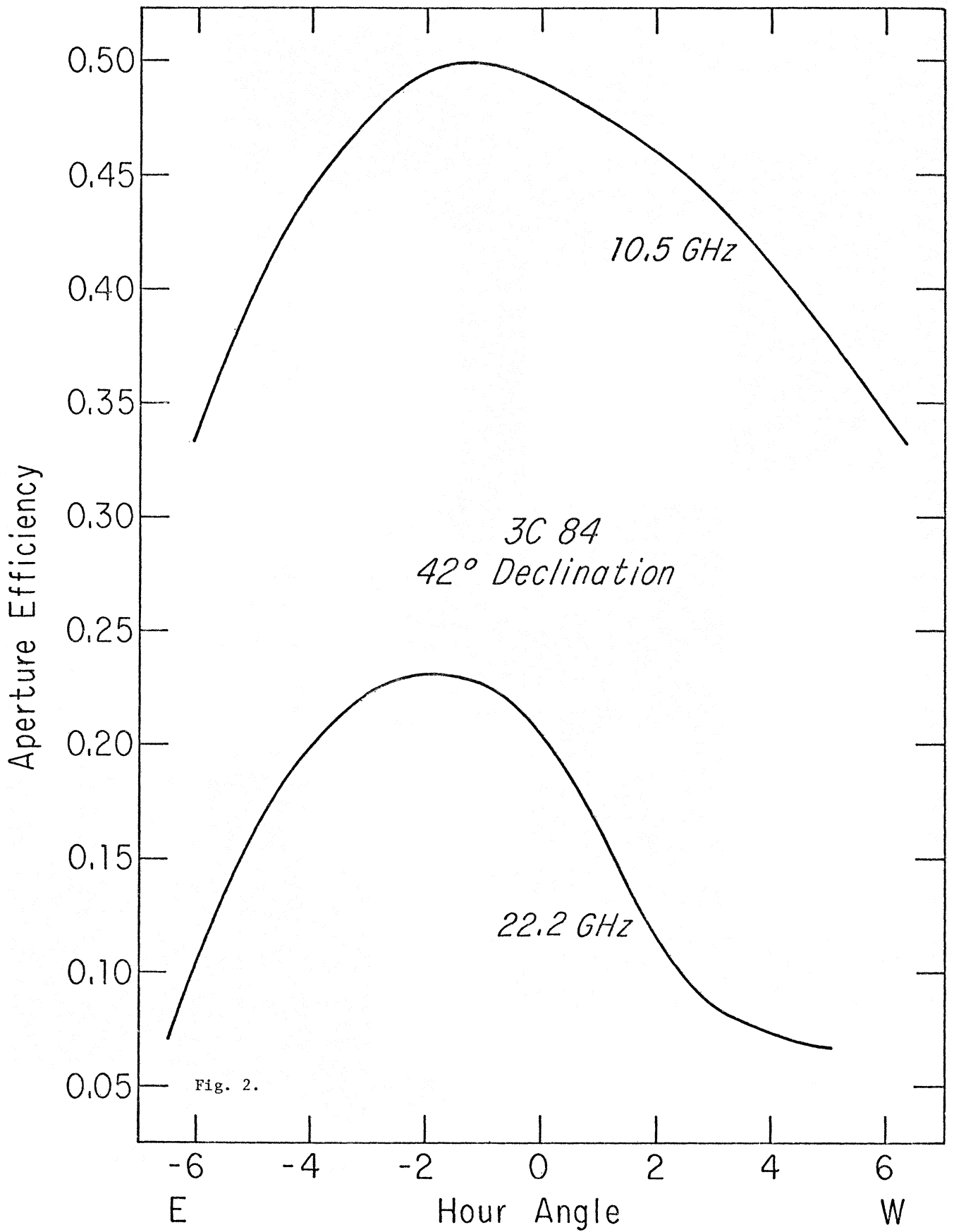
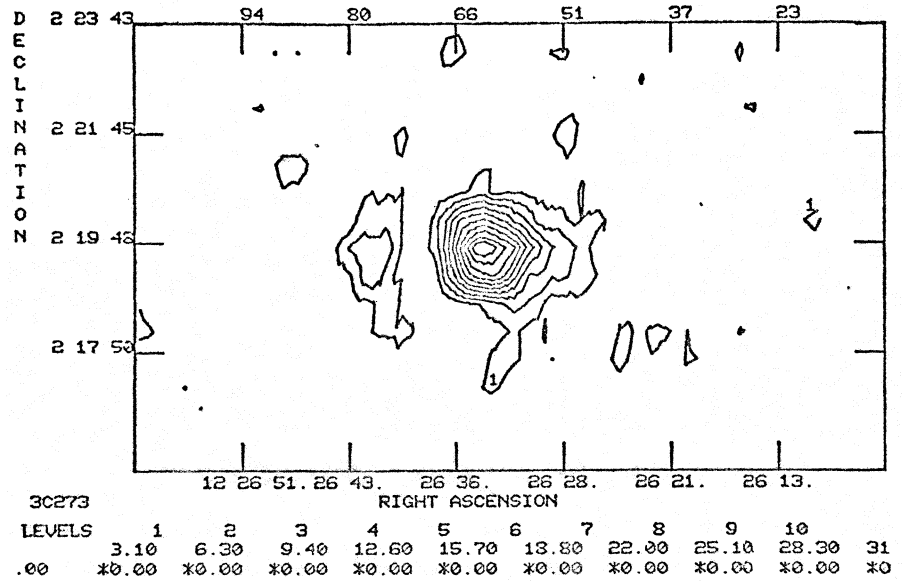


Fig. 2.

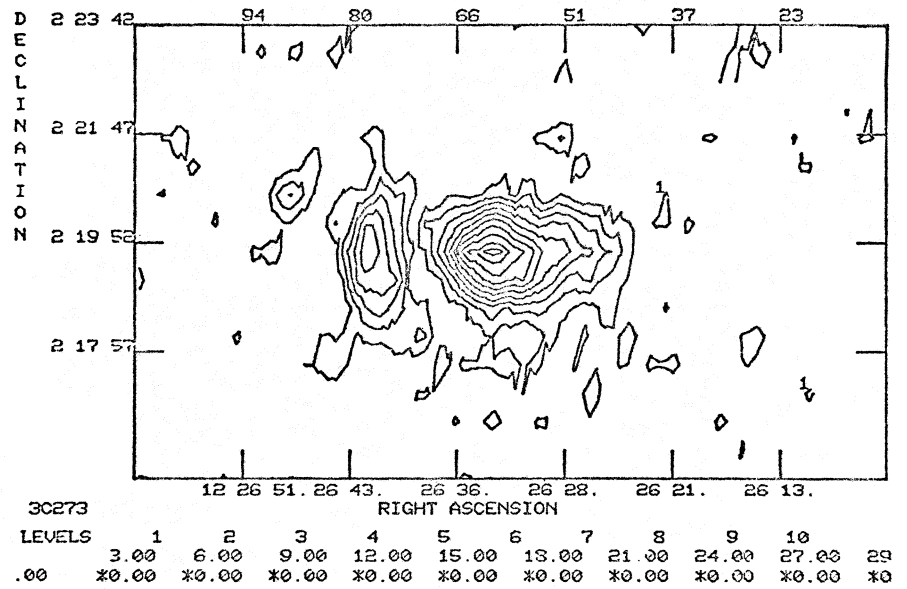
WEST
 $1^H 20^m$

Fig. 3g.



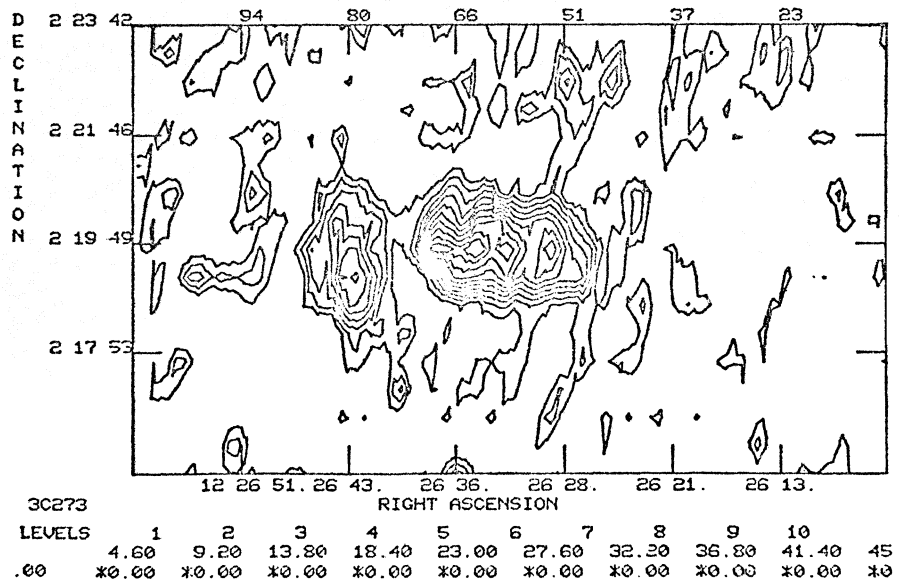
WEST
 $2^H 20^m$

Fig. 3h.



WEST
 $3^H 10^m$

Fig. 3i.



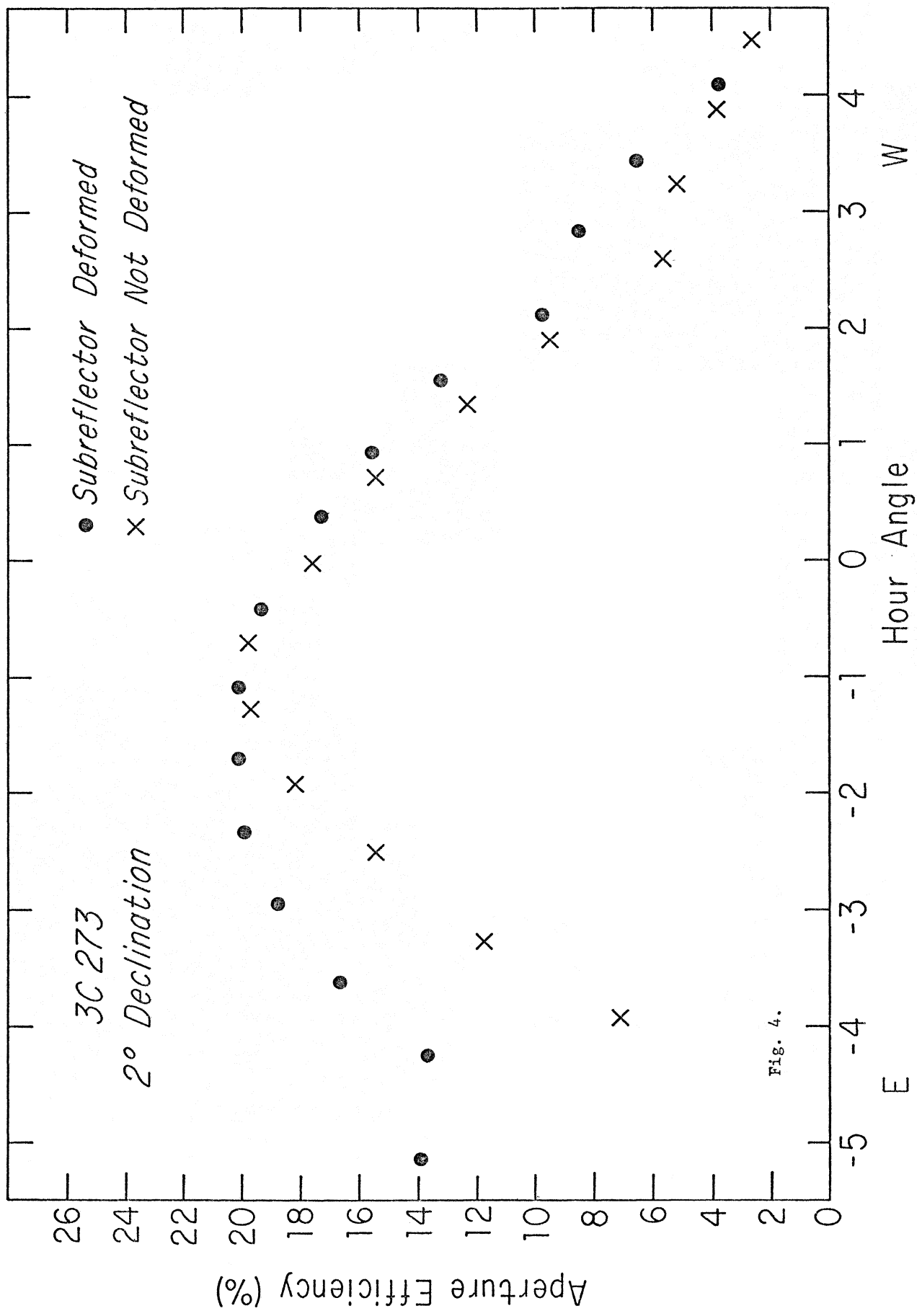


Fig. 4.

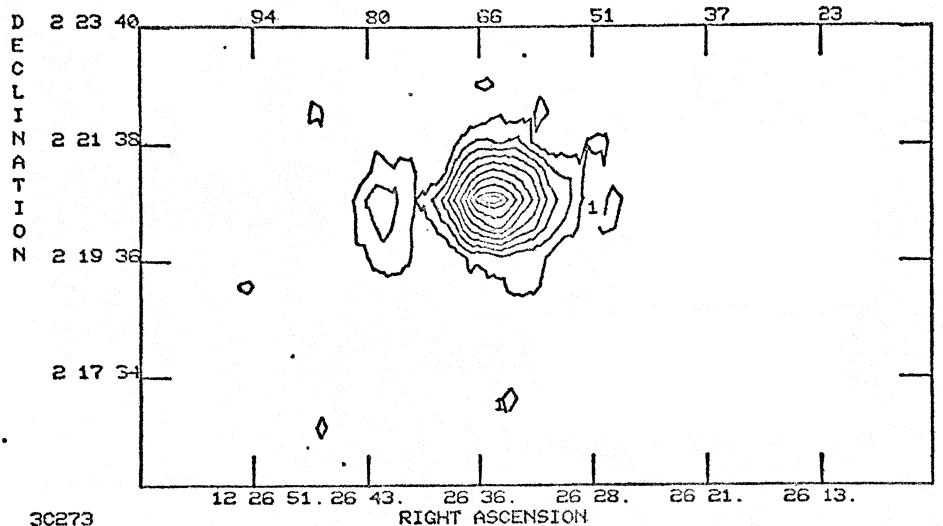


Fig. 5a.

3C 273

LEVELS	1	2	3	4	5	6	7	8	9	10
.50	5.60	11.30	17.00	22.60	28.20	33.90	39.60	45.20	50.80	53
	*0.00	*0.00	*0.00	*0.00	*0.00	*0.00	*0.00	*0.00	*0.00	*0

UNDEFORMED

3C 273 0^H 20^m WEST

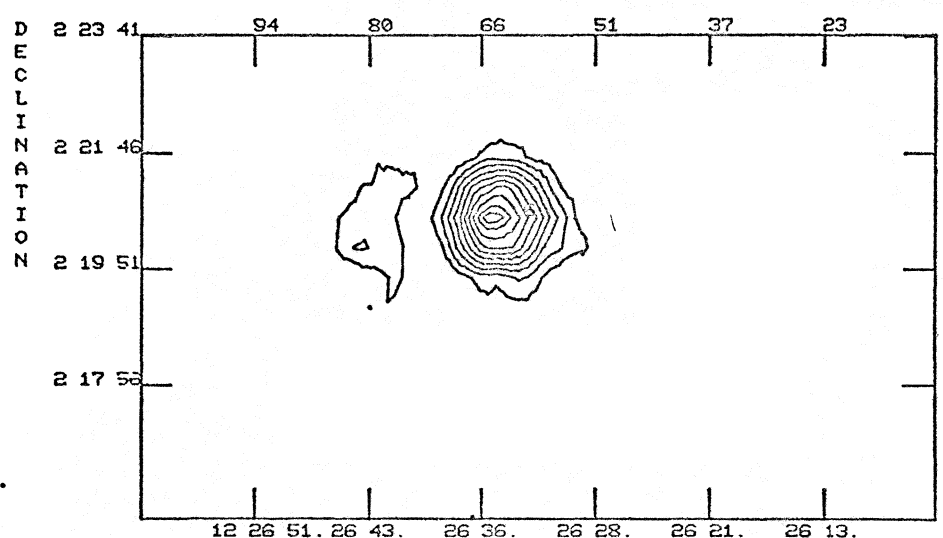


Fig. 5b.

3C 273

LEVELS	1	2	3	4	5	6	7	8	9	10
.00	10.20	20.30	30.50	40.60	50.80	61.00	71.10	81.30	91.40	98
	*0.00	*0.00	*0.00	*0.00	*0.00	*0.00	*0.00	*0.00	*0.00	*0

DEFORMED

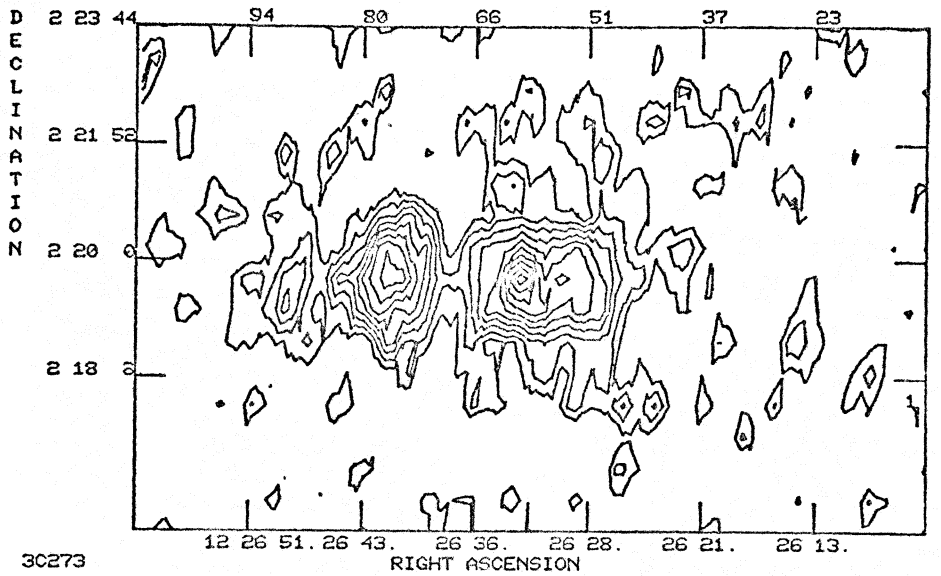


Fig. 6a.

30273

LEVELS	1	2	3	4	5	6	7	8	9	10	20
.00	*0.00	*0.00	*0.00	*0.00	*0.00	*0.00	*0.00	*0.00	*0.00	*0.00	*0.00

UNDEFORMED

30 273 2^H 20^m WEST

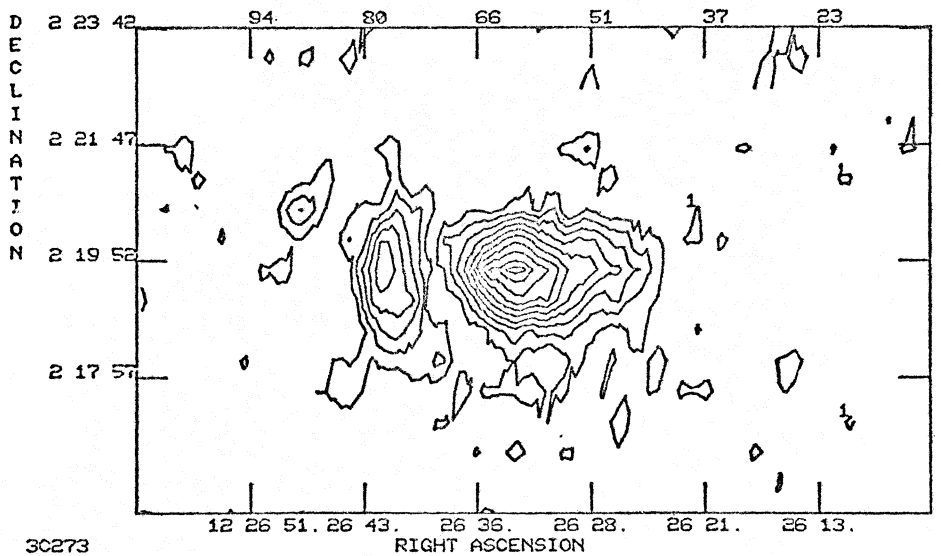


Fig. 6b.

30273

LEVELS	1	2	3	4	5	6	7	8	9	10	29
.00	*0.00	*0.00	*0.00	*0.00	*0.00	*0.00	*0.00	*0.00	*0.00	*0.00	*0.00

DEFORMED